COMPRESSION AND RAREFACTION WAVES IN SHOCK-COMPRESSED METALS

A. N. Dremin and G. I. Kanel'

UDC 532.593

The behavior of duralumin and copper is studied under conditions of specimen loading by two successive shock waves and during unloading after the shock compression. The amplitude of the first shock wave was 150-250 kbar. Direct measurements were performed of the difference in main stresses behind the shock front in duralumin. The results obtained do not agree with existing concepts of the behavior of solids under dynamic loading. Possible causes of this divergence are considered.

According to existing concepts [1-3] the stressed state of metals behind a shock front corresponds to the yield point at a given pressure. Under further compression the material should behave in an especially plastic manner, with the velocity of weak compression waves determined by the volume speed of sound. In the unloading wave there should appear an elastic precursor with amplitude exceeding the dynamic limit of elasticity at fixed pressure by a factor of two. This study will offer an experimental investigation of repetitive shock compression and viscoelastic unloading of duralumin D16 and copper M2.

1. Discontinuous Metal Loading

In the experiments on repetitive compression, specimen loading was performed by collision of an aluminum plate (10 mm thick), driven by an explosive apparatus [4] to a velocity of 2.3 ± 0.1 km/sec. At the moment of collision the plane area had a diameter of 62 ± 2 mm, and the shock wave was introduced into the specimen through a Plexiglas screen 6-8 mm thick. Since the dynamic rigidity of the Plexiglas is significantly lower than that of the striker and specimen, multiple reflection of the shock wave occurs in the screen from the boundaries with the striker and specimen, as a result of which the compression wave in the specimen initially has a stepped pressure profile. Using manganin sensors [5], the pressure profile in the specimen at various distances from the screen was recorded. Thickness of sensors, including insulating films, was 0.10-0.12 mm, initial resistance 2-2.5 Ω, and sensitive element area ~7 × 7 mm^2. Signals were recorded with a bridge circuit, with a sensor current of 8 A. The pressure behind the first shock front in duralumin was 181 ± 5 kbar; in copper, 255 ± 7 kbar. The second compression wave amplitudes were 19.5 ± 2 and 53 ± 3 kbar, respectively. The sensors were located between specimen plates in a slit whose plane was perpendicular to the direction of compression, i.e., rather than pressure in the specimen, stress in the direction of compression σ_x was measured.

Two series of experiments were performed with this configuration of the equipment. In the first series simultaneous recordings were made of two complete profiles $\sigma_x(t)$ using a two-trace oscilloscope and two sensors located at some (known) distance from each other along the specimen axis. Figure 1a shows the oscillogram of one experiment of this series, in which the stress profiles were recorded at distances h = 4 and 12 mm from the screen. The arrows on the oscillogram denote passage of the second compression wave front through the sensors. From the elapsed time between these points and the known distance between sensors the velocity of the second compression wave front was calculated. Corrections were made for nonperpendicularity of the oscilloscope beam deviation axes and the thickness of the sensor insulation. The circle in the first profile indicates a pressure flare caused by reflection from the screen of the unloading wave, appearing in the specimen after exit of the shock front into the first sensor insulation. This reflected pressure pulse makes it impossible to record the front of the second compression wave at small distances from the screen.

Moscow. Translated from Zhurnal Prikladnoi Mekhaniki i Tekhnicheskoi Fiziki, No. 2, pp. 146-153, March-April, 1976. Original article submitted May 14, 1975.

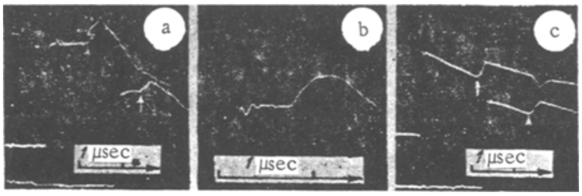

Fig. 1

In the first series, three experiments were performed for duralumin, copper, and industrial aluminum AD1. The Lagrangian velocities of the second wave front for the aluminum and copper alloys were 9.8 ± 0.2; 6.65 ± 0.1 km/sec, respectively, which correspond to the longitudinal velocity of sound in the shock-compressed material [6], within the limits of measurement error. The second shock-wave velocity, calculated with the assumption of identical shock adiabats for single and double compression, proves to be significantly less than that measured, i.e., it may be considered established that with successive compression the second wave has an elastic precursor.

For a detailed study of the profile $\sigma_x(t)$ in the second wave, experiments were performed with a more rapid oscilloscope sweep rate. Balance of the bridge containing the manganin sensor and oscilloscope gain were adjusted so that only the second wave was displayed, but with greater resolution in both time and amplitude. Figure 1b shows an oscillogram from the second series of experiments, in which recordings were made of a D16 specimen at a distance of 12 mm from the screen. The stress profiles for the second wave obtained from oscillogram processing are shown in Fig. 2a, b. The initial and final stresses were taken as the average values over a series of experiments. The time error in the profiles shown is estimated at ± 0.01 μsec, without consideration of systemic error due to sensor inertia, which is determined by insulation thickness. The fall of the first wave front in all experiments did not exceed 0.1 μsec. The second wave profile showed even qualitative variation if the striker surface proved to be curved instead of plane at the moment of impact. Convexness or concavity of the striker and shock front appear on the oscillograms as an increase or decrease in the recorded signal level. Thus, for further processing only those oscillograms were taken in which no curvature of the "shelf" after the first stress change was observed. Figure 2a shows profiles averaged over 2-3 experiments with duralumin specimens for $h_1 = 0$, $h_2 = 6$, and $h_3 = 12$ mm (curves 1-3), while Fig. 2b shows data for experiments with copper and $h_1 = 4$, $h_2 = 8$, $h_3 = 12$ mm (curves 1-3).

From the $\sigma_x(t)$ profiles thus obtained the change of state in the second wave was calculated. The complete stress jump was divided into eight equal segments. The change in degree of compression V/V_0 in each segment was determined from the expression $\Delta V/V_0 = \Delta\sigma_x/(\rho_0 a_i^2)$, where ρ_0 is the initial specimen density and a_i is the Lagrangian velocity of propagation of the average stress level for a given interval. The values a_i were determined from the profiles presented in Fig. 2 by use of the formula $1/a_i = 1/a_l + \Delta\tau/\Delta h$, where a_l is the Lagrangian velocity of the second wave front; Δh is the initial coordinate difference between neighboring sensors; $\Delta\tau$ is the difference in time intervals between the moment of passage of the second wave front through the sensor and the moment of reaching a given level σ_x in the two neighboring sensors.

Figure 3 shows the deviation of stress in the second compression wave from the original shock adiabat as a function of the degree of compression for duralumin and copper (curves 1 and 2). The shock adiabats were used in the form $D = (5.34 + 1.36u)$, km/sec for duralumin [6, 7], and $D = (3.96 + 1.5u)$, km/sec [7] for copper. As is evident from Fig. 3, all states in the second wave lie above the shock adiabat of the original material. According to classic gasdynamics [1] the final state behind the second wave front (given its stationary character) should be described on the $\sigma_x - V$ diagram of a point located below the shock adiabat of the original material. In the experiments performed here stability of the second compression wave was not attained. Preliminary specimen loading was achieved by a shock wave with rectangular pressure profile.

We will consider the character of the second wave in the case of a falling profile $\sigma_x(t)$ behind the first shock front. Figure 1c shows an experiment in which loading of a D16 specimen was achieved by a contact charge of TNT with density 1.58 g/cm^3, 80 mm in diameter, and 40 mm high through a copper screen 4 mm thick. The charge was detonated by an explosive lens. The first stress sensor was located between the copper screen and the sample, the second at a distance of 10 mm from the screen. The amplitude of the first shock wave falls from 169 to 140 kbar over the distance between sensors, while the stress before the second wave front (denoted by arrows on the oscillogram) is 105-110 kbar. The Lagrangian velocity of the second wave front in this experiment was 8.15 ± 0.1 km/sec. The longitudinal Lagrangian velocity of sound at a pressure of 105 kbar is 8.3 km/sec, while volume velocity is 7.05 km/sec, i.e., the measured velocity of the second wave front in this experiment approaches the longitudinal speed of sound. Stress rise time for the second wave increases over the intersensor distance from 0.20 to 0.28 μsec.

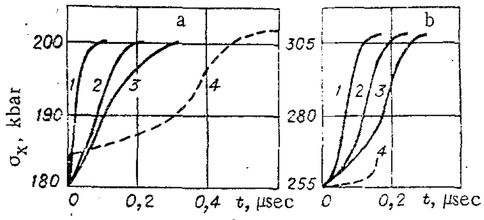

Fig. 2

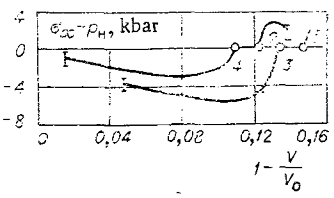

Fig. 3

2. Elastoplastic Unloading of Metals

In the experiments, recording the rarefaction wave specimen loading was done with a striker made of Plexiglas at a velocity of 3.2 ± 0.1 km/sec, with a plane central section 83 ± 2 mm. Plexiglas was chosen for the striker material because the profile of the rarefaction wave caused by reflection of the shock wave from the back surface has no singularities. This permits a direct qualitative comparison of experimental profiles of $\sigma_x(t)$ within the specimen without preliminary processing and analysis. Shock-wave amplitude in duralumin was 160 ± 5, in copper, 215 ± 7 kbar. Three electrocontact sensors were installed in a 35-mm-diameter circle on the free surface of the specimen for control of curvature and measurement of shock front velocity. The sensors were connected in parallel to a capacitor discharge circuit through resistances of 100-150 Ω. The second oscilloscope channel recorded capacitor discharge current upon closure of the contact sensors. Only those oscillograms in which time delay between curvature sensor switch-ons was less than 0.1 μsec were processed further.

Figure 4a-c shows oscillograms with recording at a distance of 10 mm from the collision surface in copper, duralumin, and (for comparison) industrial aluminum AD1. All oscillograms clearly show an elastic precursor, but we can speak of an elastic wave of finite amplitude only in duralumin.

In processing the experimental oscillograms, consideration was made of hysteresis in the dependence of manganin sensor resistance on pressure. The residual sensor resistance change (hysteresis) found in recording unloading waves from the free specimen surface was 5-6% of the total amplitude. The relationship between resistance change and the quantity σ_x in unloading was taken as linear.

Figure 5 presents Lagrangian velocity of propagation a_σ of fixed stress values as a function of the quantity σ_x for duralumin and copper (curves 1 and 2). Sensors were located 4-15 mm from the collision surface. The error in determination of a_σ does not exceed ±2%. The dependence of a_σ on coordinate does not exceed the limits of measurement error. Also shown are the Lagrangian volume velocity of sound as a function of pressure (dashed lines), calculated from the formula $a(c_0^2 + 4bp/\rho_0)^{1/2}$, assuming coincidence of shock adiabats and isentropy of unloading, in coordinates p, u [6] for duralumin and copper (curves 3 and 4). Here c_0 and b are coefficients of the linear expression for shock adiabat $D = c_0 + bu$; ρ_0 is the initial specimen density. Figure 3 shows the deviation of the unloading curve from the shock adiabat for duralumin and copper (curves 3 and 4). The unloading curves are located below the shock adiabat, which agrees with the viscoplastic model [2, 3].

3. Difference in Major Stresses behind the Shock Front.

The relative positions of unloading and secondary compression curves with respect to the shock adiabat do not correspond with accepted concepts of the process of deformation in a shock wave. Thus, additional experiments were undertaken to determine the difference in major stresses behind the shock front. In these experiments two mutually perpendicular slits were made in the specimen and filled with insulating material. Within the slits at an identical distance from the collision surface (8 mm) manganin sensors were installed. The sensors had a Π-shaped form, with the sensitive element in the crossbar region. After multiple reflections in the slit oriented perpendicular to the compression direction, there is established a pressure behind the shock front equal to the stress σ_x in perpendicular directions. Recording was done so as to simultaneously measure signals from both sensors and directly determine the difference in sensor indications [5]. Specimen loading was by collision of an aluminum plate 10 mm in diameter at a velocity of 1.85 ± 0.1 km/sec.

The experiments revealed that it was difficult to ensure sufficient reliability in the indications of the σ_y sensor, evidently because of flow instability in the slit perpendicular to the shock front and filled with a material with dynamic rigidity differing from the specimen. Thus, no reliable result was obtained for copper. For duralumin the measured stress difference behind a shock front with amplitude 170 kbar was found to be $\sigma_x - \sigma_y = 1.0 \pm 0.5$ kbar. This result is averaged over three experiments with sensor insulation being com-

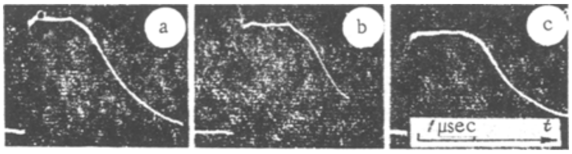

Fig. 4

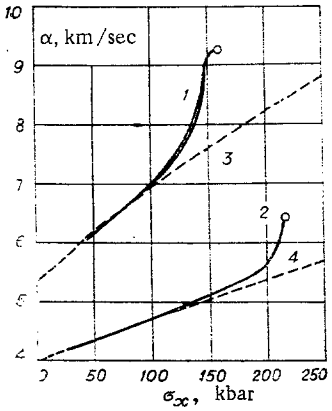

Fig. 5

posed of a set of mica plates 0.10-0.15 mm thick and Lavsan films 0.02 mm thick directly at the sensors. The total thickness of sensor and insulation was 0.25-0.35 mm.

4. Evaluation of Results

The results obtained diverge from accepted concepts of metal behavior in a shock wave in three ways: 1) for successive shock compression the second wave has an elastic precursor; 2) the final state of the material for successive compression is described by a point located above the original shock adiabat; 3) the unloading curve deviation from the shock adiabat, which for an elastoplastic material should be equal to $(4/3)(\sigma_x - \sigma_y)$ [2], reaches 5-6 kbar for duralumin, i.e., is much more than expected from the measured stress difference (0.7-2.0 kbar).

It is most probable that this divergence is related to the relaxation character of high-speed deformation. Successive compression peculiarities similar to those found in the present study have been observed at lower deformation rates. Thus, in a study of elastoplastic wave propagation in aluminum, copper, and brass wires transformed to the plastic state beforehand by shock, it was found that the front of the second (before load) impulse propagates with the velocity of elastic waves [8]. A quantitative description of stress relaxation under real conditions of shock compression (in principle) may be obtained with use of the elasto-viscous medium model considered in [9].

A second possible reason for the differences from the results expected in the elastoplastic model could be a difference in deformation mechanisms in the front of a strong shock wave and weak waves. An estimate of the maximum shear stress value in a shock front τ_{max} [10], made from the deviation of a wave ray $\sigma_x = \rho_0 D^2 (1 - V/V_0)$ from the shock adiabat, gives a result for duralumin at a shock-wave amplitude of 160 kbar τ_{max} = 11.2 kbar, and at 181 kbar τ_{max} = 14.4 kbar; for copper at 215 kbar τ_{max} = 13.9 and at 255 kbar τ_{max} = 18.3 kbar. Estimating the theoretical strength as 1/30 of the shear modulus, considering the dependence of the latter on pressure, using data of [6], gives a value of 10.5 kbar for duralumin and 16 kbar for copper; i.e., the shear stresses in the shock front are comparable to or exceed the theoretical shear strength of the material. Thus, it is not excluded that at the shock front there occurs a dislocationless supercritical shear [10], while in unloading waves and secondary compression deformation follows a dislocation mechanism and is accompanied by hardening.

In connection with this we note that an estimate of the stressed state behind the front of the first shock wave from the deviations of stress from the shock adiabat after secondary compression ($\Delta\sigma_2 \approx 2.5$ kbar) and in the unloading wave after change of the degree of compression by a value corresponding to the amplitude of the second wave ($\Delta\sigma_R \approx 4.5$ kbar) gives a value for duralumin of $\sigma_x - \sigma_y = (3/4)(\Delta\sigma_R - \Delta\sigma_2) \approx 1.5$ kbar, which agrees satisfactorily with the results of direct measurement.

We will compare the form of elastoplastic wave profiles for materials in the original state and for shock-compressed materials. In Fig. 2a (curve 4) the profile of an elastoplastic compression wave in duralumin at a distance of 12.5 mm from the collision surface is shown, constructed from data of [11]. Figure 2b (curve 4) is the profile of an elastoplastic compression wave with total amplitude of 50 kbar in high-purity polycrystalline copper at a distance of 4.0 mm [12]. One can see the qualitative similarity of the profiles in the original and shock-compressed states. For copper the elastic precursor has a triangular profile in the compression wave in the unloaded specimen, as well as in the compression waves and unloading waves in the shock-compressed material. For duralumin the elastic precursor shows a discontinuity followed by a relatively smooth change of stress both in compression of the unloaded specimen and in unloading after shock compression. The relatively low slope of the recorded secondary compression wave front apparently is determined by the inertia of the technique used.

In conclusion, the authors thank G. A. Savel'ev for his aid in the preparation and performance of the experiments.

LITERATURE CITED

1. Ya. B. Zel'dovich and Yu. P. Raizer, Physics of Shock Waves and High Temperature Hydrodynamic Phenomena, Academic Press (1966-1967).
2. L. V. Al'tshuler, M. I. Brazhnik, and G. S. Telegin, "Strength and elasticity of iron at high shock-compression pressures," Zh. Prikl. Mekh. Tekh. Fiz., No. 6, 159 (1971).
3. P. J. A. Fuller and J. H. Price, "Dynamic stress–strain release path for aluminum and magnesium measured to 200 kbar," Brit. J. Appl. Phys., Ser. 2, J. Phys. D, No. 2 (1969).
4. G. I. Kanel', A. M. Molodets, and A. A. Vorob'ev, "Projection of plates by explosion," Fiz. Goreniya Vzryva, 10, No. 6, 884 (1974).
5. G. I. Kanel' "Use of manganin sensors for shock compression pressure measurements in solid media," Article deposited at VINITI (All-Union Institute of Scientific and Technical Information), No. 477-74 (1974).
6. A. A. Vorob'ev, A. N. Dremin, and G. I. Kanel', "Dependence of coefficient of elasticity of aluminum on degree of compression in a shock wave," Zh. Prikl. Mekh. Tekh. Fiz., No. 5, 94 (1974).
7. L. V. Al'tshuler, S. B. Kormer, A. A. Bakanova, and R. F. Trunin, "The equation of state of aluminum, copper, and lead in the high-pressure region," Zh. Éksp. Teor. Fiz., 38, No. 3, 790 (1960).
8. B. M. Malyshev, "An experimental study of elastoplastic wave propagation," Zh. Prikl. Mekh. Tekh. Fiz., No. 2, 104 (1961).
9. S. K. Godunov and N. S. Kozin, "Shock-wave structure in an elastoviscous medium," Zh. Prikl. Mekh. Tekh. Fiz., No. 5 (1974).
10. G. R. Gowan, "Shock deformation and the limiting shear strength of metals," Trans. Metal. Soc. AIME, 233, No. 6, 1121 (1965).
11. J. N. Johnson and L. M. Barker, "Dislocation dynamics and steady plastic wave profiles in 6061-T6 aluminum," J. Appl. Phys., 40, No. 11, 4321 (1969).
12. O. E. Jones and J. D. Mote, "Shock induced dynamic yielding in copper single crystals," J. Appl. Phys., 40, No. 12, 4920 (1969).